THE UNSTEADY PRESSURE SIGNATURE OF TRANSONIC SHOCK WAVE/BOUNDARY LAYER INTERACTION

M. Bernardini* , S. Pirozzoli* , F. Grasso**
*** Università di Roma 'La Sapienza', Dipartimento di Ingegneria Meccanica e Aerospaziale**
Via Eudossiana 18, 00184, Roma (Italy),
**** Cnam, Chair of industrial aerodynamics, 15, rue Marat, Saint-Cyr-l'Ecole 78210 (France)**

Keywords: *Transonic flows; Shock/boundary layer interaction; Pressure fluctuations; Direct numerical simulation*

Abstract

The statistics of wall pressure fluctuations beneath a turbulent boundary layer interacting with a normal shock wave are investigated exploiting a direct numerical simulation (DNS) database. In the zero-pressure-gradient region upstream of the interaction pressure statistics well compare with canonical boundary layers in terms of fluctuation intensities and frequency spectra. Pressure fluctuations attain large values across the interaction zone, with an increase of about 7 dB from the upstream level. The main effect of the interaction on the frequency spectra is to promote the low-frequency Fourier modes, and to inhibit the high-frequency ones. Excellent collapse of frequency spectra is observed past the interaction zone when data are scaled with the local boundary layer units. In this region an extended $\omega^{-7/3}$ *power-law behavior is observed, associated with the suppression of mean shear caused by the imposed adverse pressure gradient.*

1 Introduction

The importance of interactions between shock waves and turbulent boundary layers (SBLI) in aeronautical and aerospace applications is widely recognized, since the occurrence of localized fluctuating pressure loads across the interaction region can negatively affect the lifetime of aircraft structures [1]. Especially relevant is the research on interactions occurring in the transonic regime, having an impact on the design of high-speed wings and diffuser, ad well as of turbomachinery components. Despite its relevance in practical applications, the unsteady wall pressure signature of transonic SBLI has not been investigated in detail, and most studies have focused on the unsteady pressure signature for flows with global, low-frequency motion of the impinging shock [2; 3], that is relevant for the prediction of transonic buffet on airfoils [4; 5].

At present, most of the available information on the effect of adverse pressure gradients on the wall pressure stems from investigations of low-speed boundary layers. Measurements of surface pressure fluctuation spectra for a separated turbulent boundary layer under adverse pressure gradient were reported by [6], who found that pressure fluctuations increase monotonically through the APG region, and showed that the maximum turbulent Reynolds shear stress is the proper scale for normalization. A similar conclusion was also reached by [7], who investigated the structure of wall pressure fluctuations from a DNS database of turbulent boundary layer over a flat plate. In the case of extended flow separation, the frequency spectra were found to exhibit distinct power-law scalings in different regions of the flow (upstream, within and past the separation bubble).

The aim of the present work is to investigate the structure of the wall pressure field induced

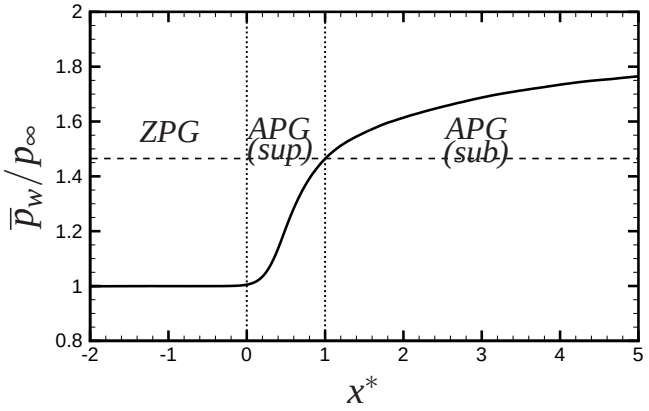

Fig. 1 Distribution of mean wall pressure as a function of the scaled streamwise coordinate x^*. The vertical lines separate three distinct regions of the flow. The horizontal line indicates the pressure corresponding to the isentropic sonic state.

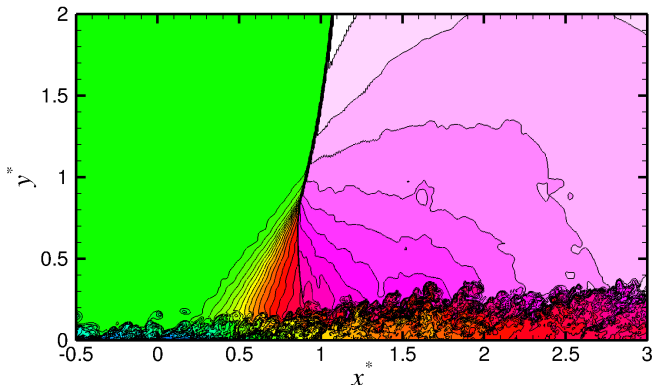

Fig. 2 Instantaneous density field in $x-y$ plane. 32 contour levels, $0.77 \leq \rho/\rho_\infty \leq 1.53$.

by a transonic shock/boundary layer interaction, providing description of the surface pressure field in terms of the frequency spectra, that are useful to predict the structural dynamical response [8]. For this purpose we interrogate a DNS database of a canonical flow case, whereby a normal shock wave is made to impinge on a turbulent boundary layer developing over a flat plate. The focus of the study is on the characterization of pressure fluctuations associated with fine-grained turbulence, and no attempt is made to investigate the possible presence of low-frequency unsteadiness that may result from self-sustained oscillations.

2 DNS database

The pressure field is analyzed exploiting the DNS database developed by the present authors [9; 10], consisting of a turbulent boundary layer that develops over a flat plate with Mach number $M_\infty = 1.3$, Reynolds number $Re_\theta = 1200$ (based on the momentum thickness of the upstream boundary layer), and made to interact with a normal shock wave. The convective terms in the Navier-Stokes equations are discretized using a hybrid approach, whereby sixth-order central discretization of the skew-symmetric split form is used in smooth regions, and shock waves are captured through a fifth-order WENO scheme, the switch being based on the Ducros sensor (see [10] for details). Viscous fluxes are computed by means of standard sixth-order central formulas, and a fourth-order Runge-Kutta method is used to perform time integration. Inlet conditions for the turbulent boundary layer are based on the rescaling-recycling procedure developed by [11] and extended to the compressible case by [12]. The mean field is kept constant at the inflow station, and fluctuations are recycled from a cross-stream slice, after suitable rescaling.

In the presentation of the results the origin of the longitudinal coordinate is set at the beginning of the interaction (x_0), corresponding to the point where the mean wall pressure starts to rise (see Fig. 1). Coordinates are normalized by the interaction length scale L, defined as [13] the distance between the streamwise station where the mean wall pressure is equal to the critical value and the origin of the interaction (indicated with x_0). Scaled coordinates are therefore denoted as $x^* = (x - x_0)/L$, $y^* = y/L$ and $z^* = z/L$. The computational region is ideally divided in three zones: i) the zero-pressure gradient region (ZPG) upstream of the interaction (for $x^* < 0$); ii) the supersonic adverse-pressure-gradient (APG) region (for $0 < x^* < 1$) and the subsonic adverse-pressure-gradient region (for $x^* > 1$).

The interaction pattern (see Fig. 2) consists of a fan of compression waves originating upstream of the nominal impingement point, and of a nearly normal shock that drives the incom-

Station #	x^*	$\overline{p}_w/p_\infty$	ρ_e/ρ_∞	u_e/u_∞	δ/δ_0^*	δ^*/δ_0^*	δ_0^*/δ_ν
0	-0.2	1	1	1	4.58	1	73.67
1	0.6	1.27	1.16	0.89	5.87	1.70	46.90
2	2.0	1.61	1.40	0.74	9.84	4.63	26.92
3	4.0	1.74	1.47	0.69	11.88	4.83	46.88

Table 1 Boundary layer properties at various streamwise stations. Subscripts: e indicates properties at the edge of the boundary layer, w indicates wall properties, 0 indicates properties taken at station 0, and ∞ free-stream properties.

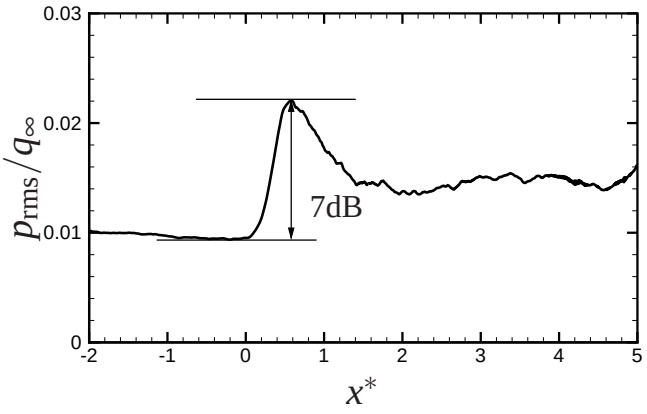

Fig. 3 Distribution of the r.m.s. wall pressure fluctuations scaled by the reference dynamic pressure q_∞.

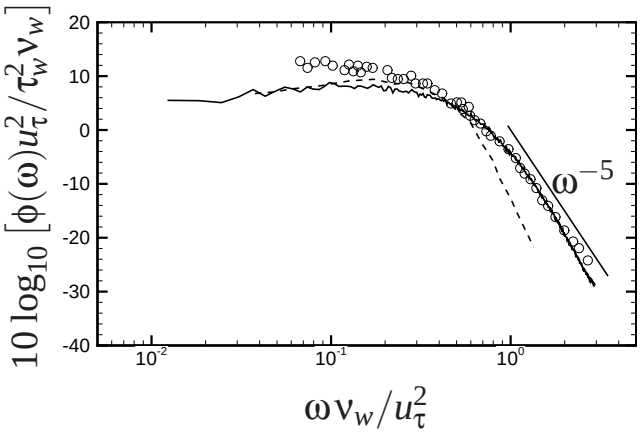

Fig. 4 Wall pressure frequency spectrum at station 0 (solid line) scaled in inner variables, compared with the experimental data of [15] at $Re_\theta = 1577$ (circles) and the DNS data of [7] at $Re_\theta = 300$.

ing flow to subsonic conditions. Past the interaction zone the flow is characterized by the the formation of a turbulent mixing layer, with unsteady release of large eddies. The analysis of the flow recovery process past the interaction zone shows that the boundary layer reacts to the impose adverse pressure gradient by attaining a new equilibrium state over a distance of O(L) past $x^* = 1$, which is characterized by self-similarity of the mean velocity field in the scaling of [14]. The DNS data were validated through comparison with experimental measurements in a transonic channel [13].

In the following the pressure statistics are reported at various streamwise stations, listed in Table 1, together with the corresponding boundary layer parameters.

3 Results

The r.m.s. of wall pressure fluctuations (p_{rms}) is reported in Fig. 3, normalized by the free-stream dynamic pressure $q_\infty = 1/2\,\rho_\infty u_\infty^2$. The distribution of p_{rms} at the wall exhibits a nearly flat distribution in the ZPG region, where $p_{\rm rms} \approx 0.010\,q_\infty$, corresponding to a sound pressure level (SPL) of about $155\,dB$ (assuming free-stream atmospheric pressure). In terms of wall units, the pressure fluctuation intensity is very nearly $p_{\rm rms} = 2.50\,\tau_w$, in good agreement with the findings of [16], who reported $p_{\rm rms} = 2.55\,\tau_w$ for low-speed turbulent boundary layers at $Re_\tau \leq 333$. Pressure fluctuations experience strong amplification in the supersonic APG region, attaining a peak value $p_{\rm rms} \approx 0.022\,q_\infty$ (corresponding to approximately 162.5 dB) at $x^* \approx 0.6$, and relax towards a nearly constant value ($0.0145\,q_\infty$) in the

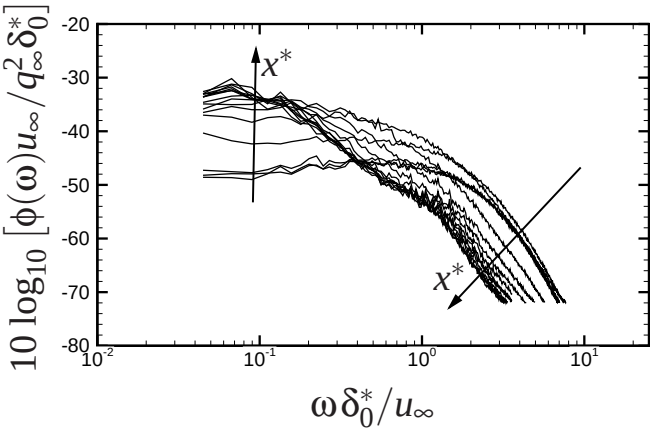

Fig. 5 Wall pressure frequency spectra at various stations scaled in outer variables taken upstream of the interaction. The arrows denote the direction of increasing x^*.

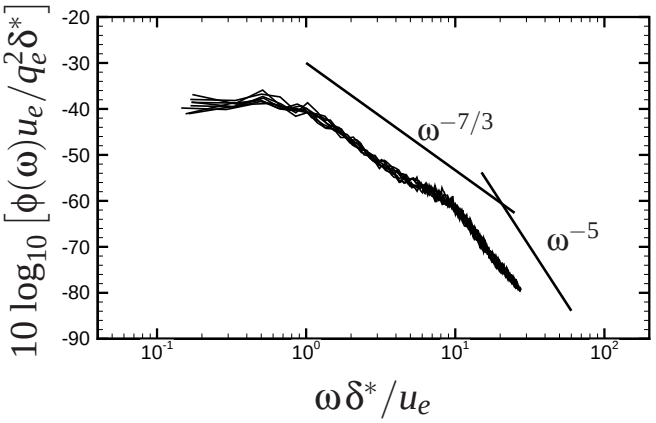

Fig. 6 Wall pressure frequency spectra at various stations in the subsonic APG region. Outer variable scaling with pressure scaled by q_e^2 (a) and τ_m^2 (b).

subsonic APG region. Amplification of pressure fluctuations in the presence of shear layers was also reported for separated low-speed turbulent boundary layers [6; 7]. To investigate the individual contributions of different Fourier modes to the r.m.s. wall pressure we have computed the one-point frequency spectrum ($\phi(\omega;x,y)$). The shape of the frequency spectrum in the ZPG region, reported in Fig. 4 well conforms to that found in incompressible boundary layer experiments [15], whereas differences are found from previous DNS at lower Reynolds number [7]. As theoretically predicted [8], the spectra drop off as approximately ω^{-5} at high frequency. The incompressible low-frequency scaling ω^2 is not observed here, either due to the limited duration of the time sample (this is true of all DNS studies published so far), or to the effect of finite compressibility, that should imply a flat spectrum at low frequencies [17]. The intermediate ω^{-1} scaling associated with turbulent activity in the log layer [18], is not observed in the present data.

In Fig. 5 the frequency spectra across the interaction zone are reported in outer scaling. Note that, to compare data from different stations, the units are referred to the reference state upstream of the interaction (station $\boxed{0}$). As found for low-speed boundary layer flows in adverse pressure gradient [19; 7], as well as for the flow past a forward-facing step [20], the shock wave enhances the lower frequencies and inhibits the higher ones, indicating the occurrence of large-scale dynamics past the interacting shock. The frequency spectra in the downstream subsonic-APG region are reported in Fig. 6, where data are normalized using the local free-stream velocity (u_e) and dynamic pressure (q_e). Excellent collapse of data is observed using this scaling, thus confirming the self-similar structure of the boundary layer recovery region as far as the mean flow properties are concerned [9]. In this zone the spectra still exhibit a ω^{-5} high-frequency scaling, but an extended $\omega^{-7/3}$ power-law scaling also appears at intermediate frequencies, followed by a spectral bump associated with the change of slope of the PSD. A $\omega^{-7/3}$ spectral scaling was first theoretically predicted by [21] for locally isotropic turbulence, as the counterpart of the Kolmogorov $k^{-5/3}$ energy spectrum scaling. Such inertial pressure scaling has been occasionally observed in experiments of turbulent jets [22] and forward-facing step flows [20], and in DNS of isotropic turbulence at large Reynolds number [23; 24]. Note that a $\omega^{-7/3}$ is not observed in ZPG boundary layers (even at very large Reynolds numbers), owing to the influence of the mean shear [25]. To our knowledge, the $\omega^{-7/3}$ has never been observed in DNS of wall-bounded turbulence, even though a narrow power-law spectral scaling (with exponent close

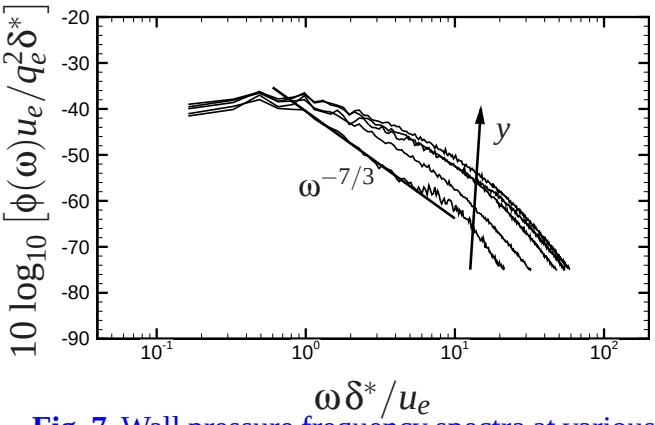

Fig. 7 Wall pressure frequency spectra at various wall-normal locations at station 2. The arrow indicates the direction of increasing y.

to -2) was reported by [7]. As seen in Fig. 7, the power-law spectral scaling is lost moving away from the wall, entering the mixing layer area.

To understand the physical significance of the observed spectral scalings we consider Lighthill's equation for the instantaneous pressure under the assumption of weak compressibility effects, upon neglect of both entropy fluctuations and viscous effects, that reads [8]

$$\frac{1}{\bar{c}^2}\frac{\partial^2 p}{\partial t^2}-\frac{\partial^2 p}{\partial x_j x_j}=\frac{\partial^2}{\partial x_i \partial x_j}\left(\rho u_i u_j\right), \qquad (1)$$

where $\bar{c}$ is a reference speed of sound. Introducing Favre decomposition into (1) yields

$$\frac{1}{\bar{c}^2}\frac{\partial^2 p'}{\partial t^2}-\frac{\partial^2 p'}{\partial x_j x_j}=\frac{\partial^2}{\partial x_i \partial x_j}\left(T_{ij}^{M-T}+T_{ij}^{T-T}\right), \qquad (2)$$

where

$$T_{ij}^{M-T}=\bar{\rho}\left(\tilde{u}_i u_j''+u_i''\tilde{u}_j\right), \qquad (3)$$

accounts for the interaction between mean velocity gradients and turbulence, and

$$T_{ij}^{T-T}=\bar{\rho}\left(u_i''u_j''-\overline{u_i''u_j''}\right), \qquad (4)$$

accounts for turbulence-turbulence interactions. The distributions of the r.m.s. source terms $S^{M-T}=T_{ij,ij}^{M-T}$, $S^{T-T}=T_{ij,ij}^{T-T}$, are reported in Fig. 8 at the stations 0 and 2, as a function of the wall distance. In the ZPG region (station 0) the M-T and the T-T source terms have comparable magnitude throughout the boundary layer,

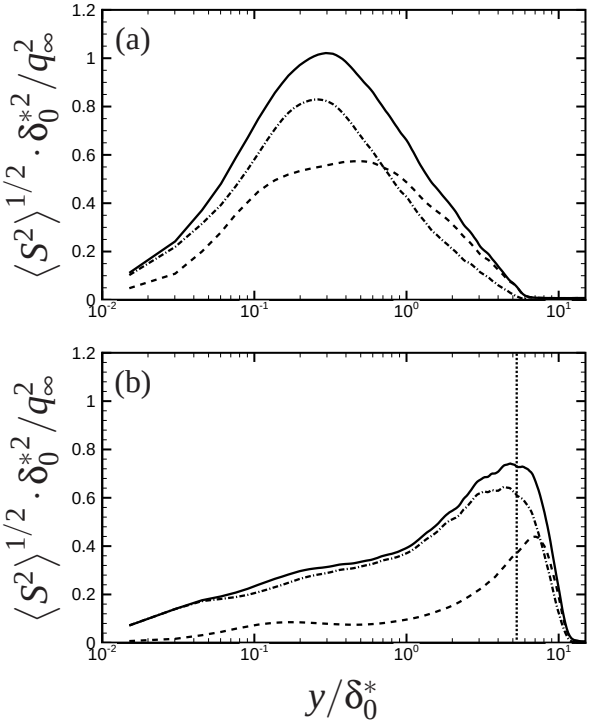

Fig. 8 Distribution of r.m.s. of pressure sources in (a) ZPG region at station 0 and (b) mixing layer region at station 2. Solid line, total source; dashed line, M-T source, dotted line, T-T source.

the former attaining a peak at $y^+\approx 36$, and the latter peaking at $y^+\approx 18$, and being dominant in the near-wall region. In the subsonic APG region (station 2) the T-T source term is dominant, and it peaks near the mid-line of the mixing layer. The M-T term stays much smaller that the T-T term through the inner part of the boundary layer, and it only becomes similar in magnitude in the outer part of the mixing layer. Taking into account these evidences, we argue that the power-law spectral scaling of wall pressure observed past the shock is related to the reduction of the mean shear caused by the adverse pressure gradient, that makes dominant the contribution of the turbulence-turbulence interaction. However, moving away from the wall, the importance of the M-T source terms again becomes non negligible, and the $\omega^{-7/3}$ scaling is not observed, as seen in Fig. 7).

4 Conclusions

The wall pressure signature of a transonic shock/boundary layer interaction has been analyzed upon interrogation of a DNS database. The structure of the pressure field upstream of the interaction is found to conform well with available experimental and DNS data, with a clear ω^{-5} scaling at high frequency. The main effect of the interaction with the impinging shock is the enhancement of low frequencies, and suppression of the higher ones, with an overall increase, mostly limited to the supersonic part of the interaction. In the downstream recovery region the pressure spectra exhibit self-similarity when plotted in local boundary layer units, and a distinct $\omega^{-7/3}$ spectral range emerges. The analysis of the pressure source terms has shown that such scaling is due to reduction of the mean shear caused by the imposed adverse pressure gradient, which makes the turbulence-turbulence source term dominant throughout the recovery region.

Acknowledgments

The support of the CASPUR computing consortium through the 2009 Competitive HPC Grant "Extremely large scale simulation of transonic turbulent flows" is gratefully acknowledged.

References

[1] D. Dolling, Fluctuating loads in shock wave/turbulent boundary layer interaction: tutorial and update, AIAA Paper 93-0284, AIAA (1993).

[2] R. Bur, R. Benay, A. Galli, P. Berthouze, Experimental and numerical study of forced shock-wave oscillations in a transonic channel, Aerosp. Sci. Tech. 10 (2006) 265–278.

[3] P. Bruce, H. Babinsky, Unsteady shock wave dynamics, J. Fluid Mech. 603 (2008) 463–473.

[4] B. H. K. Lee, Transonic buffet on a supercritical airfoil, Aeronaut. J. 94 (1990) 143–152.

[5] S. Deck, Numerical simulation of the transonic buffet over a supercritical airfoil, AIAA J. 43 (2005) 1556–1566.

[6] R. L. Simpson, M. Ghodbane, B. E. McGrath, Surface pressure fluctuations in a separating turbulent boundary layer, J. Fluid Mech. 177 (1987) 167–186.

[7] Y. Na, P. Moin, The structure of wall-pressure fluctuations in turbulent boundary layers with adverse pressure gradient and separation, J. Fluid Mech. 377 (1998) 347–373.

[8] W. K. Blake, Mechanics of Flow-Induced Sound and Vibration, Academic, 1986.

[9] S. Pirozzoli, M. Bernardini, F. Grasso, Direct numerical simulation of transonic shock/boundary layer interaction under conditions of incipient separation, J. Fluid Mech.DOI10.1017/S0022112010001710.

[10] M. Bernardini, S. Pirozzoli, F. Grasso, The wall pressure signature of transonic shock/boundary layer interaction, J. Fluid Mech.Under review.

[11] T. Lund, X. Wu, K. Squires, Generation of turbulent inflow data for spatially-developing boundary layer simulations, J. Fluid Mech. 140 (1998) 233–258.

[12] S. Xu, M. P. Martin, Assessment of inflow boundary conditions for compressible turbulent boundary layers, Phys. Fluids 16 (2004) 2623–2639.

[13] J. Delery, J. G. Marvin, Shock-wave boundary layer interactions, Tech. Rep. 280, AGARDograph (1986).

[14] M. V. Zagarola, A. J. Smits, Mean flow scaling of turbulent pipe flow, J. Fluid Mech. 373 (1998) 33–79.

[15] S. P. Gravante, A. M. Naguib, C. E. Wark, H. M. Nagib, Characterization of the pressure fluctuations under a fully developed turbulent boundary layer, AIAA J. 36 (1998) 1808–1816.

[16] T. Farabee, M. J. Casarella, Spectral features of wall pressure fluctuations beneath turbulent boundary layers, Phys. Fluids 3 (10) (1991) 2410–2420.

[17] J. E. Ffowcs Williams, Surface pressure fluctuations induced by boundary layer flow at finite mach number, J. Fluid Mech. 22 (1965) 507–519.

[18] P. Bradshaw, 'inactive' motion and pressure fluctuations in turbulent boundary layers, J. Fluid Mech. 30 (1967) 241–258.

[19] K. Cipolla, W. Keith, Effects of pressure gradients on turbulent boundary layer wave number frequency spectra, AIAA J. 38 (2000) 1832–1836.

[20] R. Camussi, M. Felli, F. Pereira, G. Aloisio, A. D. Marco, Statistical properties of wall pressure fluctuations over a forward-facing step, Phys. Fluids 20 (2008) 075113.

[21] G. Batchelor, Pressure fluctuations in isotropic turbulence, Proc. Camb. Phil. Soc. 47 (1951) 359–374.

[22] Y. Tsuji, T. Ishihara, Similarity scaling of pressure fluctuation in turbulence, Phis. Rev. E 68 (2003) 026309.

[23] T. Gotoh, R. Rogallo, Intermittency and scaling of pressure at small scales in forced isotropic turbulence, J. Fluid Mech. 396 (1999) 257–285.

[24] T. Ishihara, Y. Kaneda, M. Yokokawa, K. Itakura, A. Uno, Spectra of energy dissipation, enstrophy and pressure by high-resolution direct numerical simulations of turbulence in a periodic box, J. Phys. Soc. Jpn. 72 (2003) 983–986.

[25] Y. Tsuji, J. H. N. Fransson, P. H. Alfredsson, A. V. Johansson, Pressure statistics and their scaling in high Reynolds number turbulent boundary layers, J. Fluid Mech. 585 (2007) 1–40.

4.1 Copyright Statement